

Geochronology of the Arkansas Alkaline Province, Southeastern United States

G. Nelson Eby and Paulo Vasconcelos¹

Department of Environmental, Earth, and Atmospheric Sciences, University of Massachusetts,
Lowell, Massachusetts 01854, U.S.A.
(e-mail: nelson_eby@uml.edu)

ABSTRACT

The Arkansas alkaline province (AAP) consists of intrusive bodies ranging in lithology from carbonatite and lamproite through nepheline syenite. Apatite and titanite fission-track ages fall into two groups—101–94 Ma and ~88 Ma. New ⁴⁰Ar/³⁹Ar ages and those reported in the literature define a third age group of ~106 Ma. Apatite and titanite fission-track ages are concordant, indicating rapid cooling due to the emplacement of these intrusions at high levels during a time of regional uplift. There is a relationship between age and petrology: (1) lamproites are emplaced at ~106 Ma, (2) carbonatites and associated silica-undersaturated rocks are emplaced between 101 and 94 Ma, and (3) large nepheline syenite bodies are emplaced at ~88 Ma. Chemical and isotopic data support the inference that the lamproites are derived from subcontinental lithosphere, while the other sequences are derived from the asthenosphere. The ages for the AAP and other conflicting information do not support the hypothesis that the AAP was formed by the passage of the North American plate over the Bermuda hotspot. A more likely explanation is that the magmatism was related to extension and reactivation of faults associated with the Mississippi graben.

Online enhancement: appendix table.

Introduction

Cretaceous alkaline rocks are widespread throughout the northern Gulf of Mexico basin, southeastern United States, but are only sparsely exposed at the surface (Byerly 1991). Subsurface exposures of alkaline rocks have been encountered in drill holes in southeast Oklahoma, south-central Texas, northeast Louisiana, southeast Arkansas, and west-central Mississippi. The four major groups of subsurface volcanic and hypabyssal rocks are trachytes, phonolites, alkaline basalts, and lamprophyres (Kidwell 1951). Baksi (1997) reports ⁴⁰Ar/³⁹Ar ages for these rocks ranging from 67.2 ± 0.4 to 80.7 ± 1.3 Ma. Volcanoclastic sediments of the Woodbine Formation in southwest Arkansas primarily contain phonolite and trachyte cobbles with lesser trachybasalt cobbles. Whole-rock ⁴⁰Ar/³⁹Ar ages for these cobbles range from 92.4 ± 0.7 to 94.2 ± 0.9 Ma (Baksi 1997). The major surface ex-

posures of alkaline rocks are found in the Arkansas alkaline province (AAP), which consists of seven intrusions or intrusive complexes that lie along a northeast–southwest trend that falls on the extension of the Mississippi Valley graben (fig. 1). In this article we report new apatite and titanite fission-track and ⁴⁰Ar/³⁹Ar mica and whole-rock ages for the major intrusive bodies (with the exception of Prairie Creek) and a number of dikes from the AAP.

Geology

The various intrusions of the AAP were emplaced into the folded and faulted lower to middle Paleozoic rocks of the Ouachita Mountain fold belt. The orogenic belt is cored by the Benton uplift (Upper Cambrian to Lower Mississippian rocks) which is enclosed by Upper Mississippian and Lower Pennsylvanian rocks, all of which have been strongly folded (Arbenz 1989). The rocks of the Benton Uplift are predominately shales, clastic sandstones, cherts, and minor conglomerates (e.g., Ordovician

Manuscript received February 6, 2009; accepted June 19, 2009.

¹ Department of Earth Sciences, University of Queensland, Brisbane, Queensland 4072, Australia.

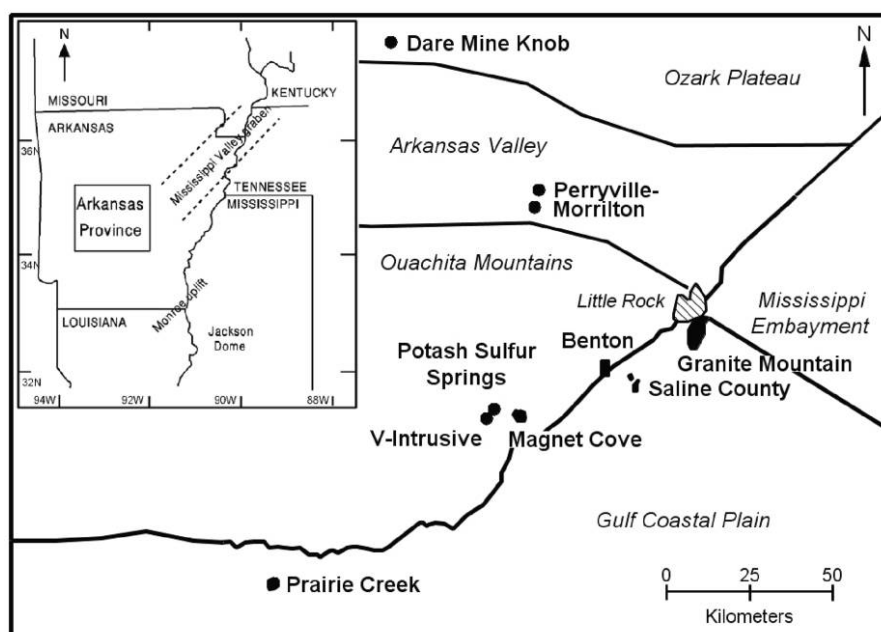


Figure 1. Regional setting for the Arkansas alkaline province and locations of the various intrusives. Modified from Morris (1987).

Womble, Mazarn, and Collier shales, Crystal Mountain and Blakely Sandstone, and Mississippian/Devonian Arkansas Novaculite). Immediately east of the Ouachita Core, an erosional surface of Middle Cretaceous age separates these rocks from the overlying Upper Cretaceous to Holocene sediments of the Mississippian embayment.

There is great petrographic diversity in the AAP (Morris 1987). Lithologies include diamond-bearing lamproite (Prairie Creek, madupitic olivine lamproite and phlogopite lamproite tuff; Mitchell and Bergman 1991, p. 46); lamproite (Dare Mine Knob); carbonatites and associated ijolites, jacupirangites, nepheline syenites, and phonolites (Magnet Cove and Potash Sulfur Springs); a variety of mafic and felsic dikes (V-intrusive and Benton dike swarm); and the nepheline syenites and syenites of the Granite Mountain and Saline County intrusions. Volumetrically, Granite Mountain and Saline County are the major intrusive complexes in the AAP. Weathering of the central Arkansas syenites during the early Cenozoic produced the Arkansas bauxite deposits, the only commercial bauxite deposits in the United States. Besides the major intrusive complexes, thin carbonatite dikes have been identified at Morrilton and Perryville (McCormick and Heathcote 1979), approximately 80 km north of the Magnet Cove complex. Besides the surface exposures, gravity (Hendricks 1988) and

magnetic (Hildenbrand 1985) data indicate the existence of large subsurface intrusions (although of uncertain lithology). Carbonatite, carbonatite-pyroxenite breccias, pyroxenite, lamprophyre, serpentinized olivine-bearing pyroxenite/peridotite, and partly altered felsic rocks were encountered in drill holes in the central Arkansas area (Saline County; Flohr and Howard 1994).

Analytical Methods

Fission-Track Ages. Apatite and titanite were separated from crushed rock samples using standard heavy liquid and magnetic separation techniques. Apatite ages were determined using the population method. Based on electron microprobe data, all the apatites dated in this study are F-rich ($F = 1.39\text{--}3.28$ wt%, and the $Cl/[Cl+F]$ ratios, using weight percent abundances of the elements, are less than 0.04). For each sample, the apatites were split into two groups. One group was annealed for 6 h at 520°C , irradiated, mounted, and polished. The irradiation was done using pneumatic system 1 of the University of Massachusetts Lowell 1-Mw swimming-pool research reactor. The nominal flux for this pneumatic system is 1×10^{12} n cm^{-2} s^{-1} , and the Cd ratio (relative to an Au monitor) is 24. The total neutron dose was monitored using NBS standard glass SRM962. The second set of unirra-

diated grains was mounted and polished. Both sets of grains were simultaneously etched for 20–25 s at room temperature in 10% HNO₃. Track densities were subsequently determined using a $\times 100$ oil-immersion objective. The zeta calibration method described by Hurford and Green (1982, 1983) and Hurford (1990) was used to calculate the fission-track ages. For this laboratory, the apatite $\zeta = 314 \pm 10$.

Titanite ages were determined using the external detector method. Titanite grains were mounted in epoxy and polished to expose an internal surface. The grains were etched for approximately 1 h at 120°C in a saturated NaOH solution. An external mica detector was affixed to each grain mount. The samples were irradiated (using the same system as for apatite). Following irradiation, the mica detectors were etched for 12 min at room temperature in concentrated HF. Fission-track densities for both the grains and the detector were determined using a $\times 100$ oil-immersion objective. For this laboratory, the titanite zeta calibration = 317 ± 6 .

Error estimates for individual ages are standard deviations based on the variation of the mean track density for the induced and spontaneous tracks and the fluence detectors. This approach probably overestimates the error associated with an individual age. When more than one age was determined for an intrusion, mean ages are reported. The analytical data are listed in table 1.

⁴⁰Ar/³⁹Ar Ages. Ages were determined for two groups of green phlogopite grains separated from a carbonatite sample (AK-11) from Magnet Cove. Total rock ages were determined for a lamproite sample (DMK-2) from Dare Mine Knob. Crushed material was ultrasonically cleaned, and 5–10 mica grains (0.5–2 mm in size) were handpicked for analysis. Rock fragments were used for the total rock ages.

The phlogopite crystals and whole-rock grains were placed in individual wells in an aluminum disk, together with grains of Fish Canyon fluence monitor following the geometry illustrated by Vasconcelos et al. (2002), and they were irradiated for 14 h at the B-1 cadmium-lined in-core irradiation tube (CLICIT) facility at the Radiation Center facility at Oregon State University. The J factors for each Al-disk were determined by the laser total fusion analyses of 15 individual aliquots of neutron fluence monitor, each consisting of 1–3 grains of Fish Canyon sanidine. Before analysis, the unknown grains and fluence monitors were baked out under vacuum at $\sim 200^\circ\text{C}$ for ~ 12 h. The grains were heated incrementally with a continuous-wave Ar-ion laser with a defocused beam. Active gases re-

leased during laser heating were removed by a -133°C cold trap and two C-50 SAES Zr-V-Fe getters. Argon isotopes in the cleaned gas fractions were analyzed in an MAP 215-50 noble gas mass spectrometer. Full system blanks and air pipettes were determined before and after each sample. The data were corrected for atmospheric contamination, nucleogenic interferences, and mass discrimination. All ages are reported using the K-decay values of (Steiger and Jäger 1977). All errors are quoted at the 2σ confidence level (95%) and include the errors in the irradiation correction factors and the error in J . The reported errors do not include the uncertainty in the age of the flux monitor or the uncertainty of the potassium decay constants. A plateau age is defined as a sequence of three or more steps corresponding to at least 50% of the total ³⁹Ar released and whose age values are within 2σ of the mean value. An integrated age is the apparent age obtained by the total gas released by a sample during the incremental-heating analyses. ⁴⁰Ar/³⁹Ar ages are reported graphically (fig. 2), and the complete data set (1σ errors) is provided in table A1, available in the online edition or from the *Journal of Geology* office.

Results

The fission-track ages fall into two groups: ~ 88 and 97–101 Ma. Mean ages for each intrusion are calculated using both the apatite and titanite ages. The younger results were obtained for the Granite Mountain (88.1 ± 1.4 Ma) and Saline County (88.4 ± 2.2 Ma) intrusions located at the southeastern end of the province (fig. 3). Other intrusions were dated by the fission-track method: V-intrusive (99.0 ± 1.9 Ma), Potash Sulfur Springs (101 ± 1.7 Ma), Magnet Cove (97.1 ± 0.8 Ma), Benton dikes (97.7 ± 0.6 Ma), and Morrilton-Perryville carbonatites (99.0 ± 0.1 Ma).

⁴⁰Ar/³⁹Ar ages were obtained for two individual grains of green phlogopite (AK-11) from the carbonatite at Magnet Cove and for two whole-rock grains from the lamproite (DMK-2) at Dare Mine Knob. The two green phlogopite grains produced well-defined plateaus whose ages (94.4 ± 1.0 and 94.1 ± 1.0 Ma) agreed within experimental error with the integrated ages (94.5 ± 1.3 and 94.0 ± 1.2 Ma). The weighted mean age for the green phlogopite, 94.3 ± 1.0 Ma, represents the age of the carbonatite at Magnet Cove. One of the lamproite rock samples yields a reliable plateau, defining an age of 106.3 ± 1.1 Ma. The other sample does not define a plateau according to the definition above, but it defines a flat segment, containing $\sim 80\%$ of

Table 1. Apatite and Titanite Fission-Track Ages

Sample, lithology, mineral dated	No. crystals	Spontaneous		Induced		Dosimeter		Age (Ma)	Mean age (Ma)
		ρ_s	(N_s)	ρ_i	(N_i)	ρ_d	(N_d)		
V-intrusive:									
AK-6:									
Microijolite:									
Apatite	50/57	3.4	408	3.42	468	3.307	2676	102.3 ± 10.1	
AK-7:									
Nepheline syenite:									
Titanite	7	3.39	57	3.16	53	5.856	3885	98.7 ± 17.9	
AK-8:									
Malignite:									
Apatite	120/120	3.89	1122	4.07	1173	3.307	2676	98.3 ± 6.5	
Titanite	10	1.75	42	1.67	40	5.849	3885	96.4 ± 17.0	
Mean apatite									100.3 ± 2.8
Mean titanite									97.6 ± 1.6
Potash Sulphur Springs:									
AK-5A:									
Carbonatite									
Apatite	200/200	.74	353	.67	318	2.989	3516	102.7 ± 9.3	
AK-5B(1):									
Ijolite:									
Apatite	100/100	2.91	698	2.97	714	3.307	2676	100.8 ± 8.0	
AK-5B(2):									
Ijolite:									
Apatite	100/100	3.43	824	3.21	771	2.989	3516	99.4 ± 8.4	
Mean apatite									101.0 ± 1.7
Magnet Cove:									
MC-1:									
Phonolite:									
Apatite	40/40	.95	91	.99	95	3.307	2676	98.7 ± 17.8	
Titanite	7	7.26	122	6.85	115	5.909	3885	98.4 ± 9.8	
MC-2:									
Jacupirangite:									
Apatite	100/100	8.42	2021	9	2160	3.307	2676	96.3 ± 8.7	
Titanite	7	8.57	144	8.16	137	5.897	3885	97.3 ± 9.7	
MC-3:									
Carbonatite:									
Apatite	100/100	10.62	2550	11.42	2741	3.307	2676	95.7 ± 6.4	
MC-4:									
P-leuc syenite:									
Titanite	4	4.58	44	4.37	42	5.880	3885	96.9 ± 22.3	
MC-5:									
Gt-pyx syenite:									
Apatite	80/44	16.1	1288	15.63	685	2.989	3516	95.8 ± 5.7	
MC-6:									
Ijolite:									
Apatite	200/200	.46	221	.45	215	2.989	3516	95.1 ± 11.7	
Titanite	10	1.42	34	1.34	32	5.869	3885	97.7 ± 36.2	
AK-9:									
Nepheline syenite:									
Apatite	50/50	1.68	202	1.63	195	2.989	3516	95.9 ± 14.4	
AK-10(1):									
Ijolite:									
Apatite	120/120	2.82	811	3	865	3.307	2676	96.7 ± 7.8	
AK-10(2):									
Ijolite:									
Apatite	100/100	2.56	615	2.48	283	2.989	3516	96.0 ± 8.4	
AK-11:									
Carbonatite:									
Apatite	100/100	4.74	1137	4.58	1100	2.989	3516	96.3 ± 17.6	
AK-12:									
Ijolite:									
Apatite	120/120	1.6	463	1.51	436	2.989	3516	98.5 ± 8.4	

Table 1. (Continued)

Sample, lithology, mineral dated	No. crystals	Spontaneous		Induced		Dosimeter		Age (Ma)	Mean age (Ma)
		ρ_s	(N_s)	ρ_i	(N_i)	ρ_d	(N_d)		
AK-15B:									
Phonolite:									
Titanite	6	28.2	406	26.3	379	5.839	3885	98.4 ± 9.9	
Mean apatite									96.5 ± 1.2
Mean titanite									97.6 ± 1.6
Benton dikes:									
AK-16:									
Camptonite:									
Apatite	120/120	2.07	595	2.17	625	3.307	2676	98.1 ± 9.7	
AK-18:									
Sannaite:									
Titanite	5	5.67	68	5.34	64	5.830	3885	97.3 ± 23.5	
Morrilton-Perryville carbonatites:									
85-59:									
Carb breccia:									
Apatite	100/100	4.98	1194	5.25	1260	3.353	2627	98.9 ± 6.7	
85-65:									
Carbonatite:									
Apatite	100/100	2.77	665	2.92	700	3.353	2627	99.0 ± 9.2	99.0 ± .1
Mean apatite									
Saline County:									
Mu-1:									
Nepheline syenite:									
Apatite	4/4	8.44	81	9.17	88	3.027	1866	86.8 ± 25.1	
Titanite	11	42.2	1113	43.4	573	2.97	1866	89.9 ± 8.6	
Granite Mountain:									
Mu-B:									
Syenite:									
Apatite	18/20	1.37	59	1.44	69	3.027	1866	89.7 ± 16.7	
Titanite	10	6.63	159	3.58	86	2.989	1866	87.1 ± 12.4	
Mu-C:									
Syenite:									
Titanite	7	3.33	56	1.78	30	2.989	1866	87.9 ± 49.4	
Mu-8X:									
Ol syenite:									
Apatite	100/100	.63	150	.66	158	3.027	1866	90.0 ± 11.2	
KL-86-11:									
Pink syenite:									
Apatite	40/40	2.31	222	2.72	261	3.333	2627	88.1 ± 9.1	
Titanite	11	3.75	99	2.27	60	3.391	2627	88.1 ± 13.0	
85-211:									
Ol syenite:									
Apatite	200/200	.51	243	.59	283	3.333	2627	89.7 ± 9.4	
86-12:									
Pink syenite:									
Apatite	21/21	3.53	178	4.27	215	3.333	2627	85.8 ± 11.7	
Titanite	8	2.71	52	1.67	32	3.372	2627	86.1 ± 13.3	
86-20:									
Pegmatite:									
Titanite	14	3.75	126	2.23	75	3.353	2627	88.7 ± 9.9	
Mean apatite									88.7 ± 1.8
Mean titanite									87.6 ± 1.0

Note. ρ = track density (10^5 tracks cm^{-2}), N = number of tracks counted; subscripts s, i, and d denote spontaneous, induced, and dosimeter, respectively. leuc = leucocratic; gt-pyx = garnet pyroxene.

the ^{39}Ar gas, that defines a plateaulike age of 106.6 ± 1.1 Ma. The integrated ages for the two grains (103.6 ± 1.4 and 104.2 ± 1.4 Ma) are slightly younger than the plateau ages, suggesting a small amount of $^{40}\text{Ar}^*$ loss for the two grains. $^{40}\text{Ar}^*$ loss

is confirmed by the ascending spectra obtained for the two grains. A probability density plot for all the individual step ages displays a relatively large scatter due to the Ar losses in the low temperature steps. However, when outlier steps are deleted, the

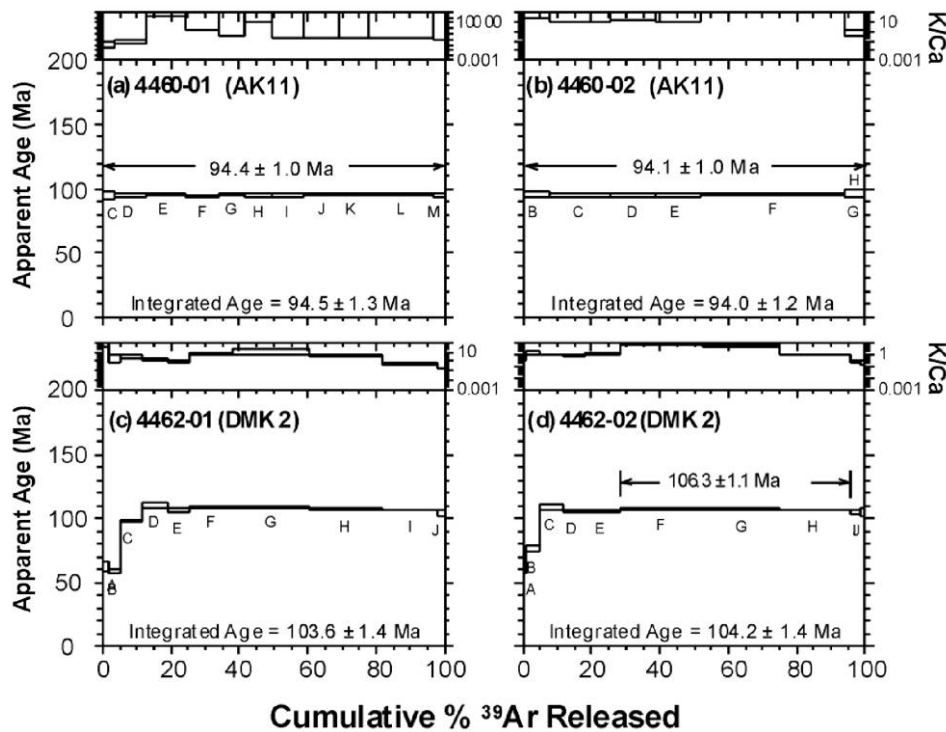


Figure 2. $^{40}\text{Ar}/^{39}\text{Ar}$ spectra (2σ errors) for AK-11 green phlogopite and DMK-2 whole rock.

population defines a well-defined age peak at 105.9 Ma, and the weighted mean age for all the steps defining this peak is 105.7 ± 1.1 Ma (MSWD = 0.68, probability = 0.60), which we define as the best age estimate for the Dare Mine Knob lamproite. This age also corresponds to the age of the isochron plotted for all the steps (age = 105.7 ± 0.6 Ma, $^{40}\text{Ar}/^{36}\text{Ar}$ intercept = 298 ± 6 , MSWD = 1.5, $n = 8$).

The distribution of fission-track ages and the $^{40}\text{Ar}/^{39}\text{Ar}$ Ar age for Magnet Cove are shown in figure 4. The $^{40}\text{Ar}/^{39}\text{Ar}$ carbonatite age is slightly younger than the apatite fission-track age for the same sample, but the ages are the same within experimental error. The silicate rocks tend to give slightly older ages than the carbonatite, in agreement with the sequence of emplacement at Magnet Cove. However, the ages are statistically indistinguishable and cannot be used to infer the sequence of emplacement. Rather, the ages indicate that all the units at Magnet Cove were emplaced in a relatively short period of time.

Ages have been reported for the AAP using a variety of radiometric dating methods (table 2). Ages obtained for the Prairie Creek lamproite range from 99 to 108 Ma. Most of these ages are suspect because the mica used to determine the age gave low

K_2O values. The notable exception is the conventional K-Ar phlogopite age of 106 ± 3 Ma reported by Gogineni et al. (1978). This age is statistically indistinguishable from the $^{40}\text{Ar}/^{39}\text{Ar}$ age (105.7 ± 1.1 Ma) determined in this study for the Dare Mine Knob lamproite. These two ages define the oldest intrusive units at the western end of the province, both of which are lamproites. For Magnet Cove, a variety of dating techniques gave ages ranging from 94 to 105 Ma (table 2). Previously determined $^{40}\text{Ar}/^{39}\text{Ar}$ ages (Baksi 1997) of 94.2 ± 0.2 and 94.4 ± 0.2 Ma are identical within error to the $^{40}\text{Ar}/^{39}\text{Ar}$ ages determined in this study. The 101 ± 1.7 -Ma apatite fission-track age for Potash Sulfur Springs is in agreement with a previously determined U-Pb zircon age of 100 ± 2 Ma (Zartman and Howard 1987). For Granite Mountain, there is excellent agreement between the titanite and apatite fission-track ages and previously determined ages (table 2), with all ages falling in the range 88–90 Ma.

Discussion

Cooling History. The fission-track and $^{40}\text{Ar}/^{39}\text{Ar}$ ages determined in this study represent the time at which the mineral(s) cooled below the blocking or closure temperature for the particular radiomet-

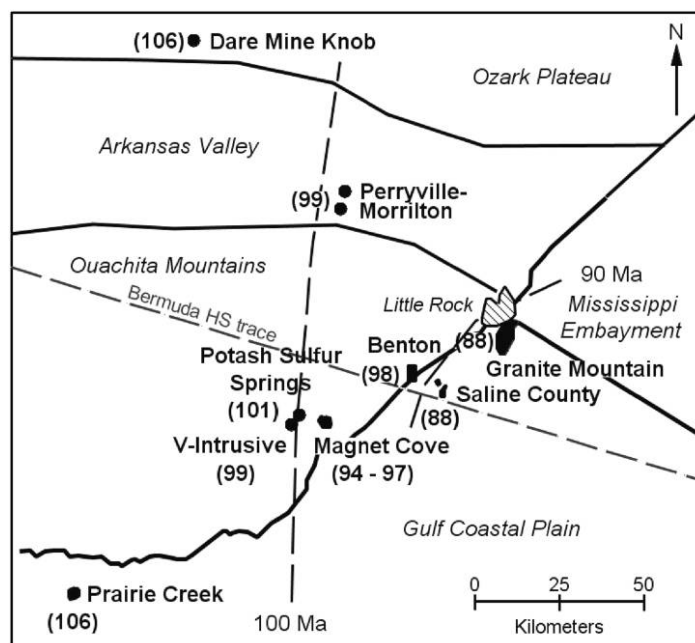


Figure 3. “Best” ages for the various intrusives of the Arkansas alkaline province. The “best” ages are derived from the ages reported in this article, the $^{40}\text{Ar}/^{39}\text{Ar}$ ages of Baksi (1997), the K-Ar Prairie Creek phlogopite age of Gogineni et al. (1978), and the U-Pb zircon age of Zartman and Howard (1987). Long dashed lines labeled 100 Ma and 90 Ma geographically divide the intrusives into three age groups. The Bermuda hotspot trace is from Morgan (1983).

ric system. For apatite, the closure temperature for fission-track retention is $100^\circ \pm 20^\circ\text{C}$ (Wagner 1968; Naeser and Faul 1969; Naeser 1981). For titanite, the closure temperature for fission-track retention is $\sim 275^\circ \pm 25^\circ\text{C}$ (Fitzgerald and Gleadow 1988). The $^{40}\text{Ar}/^{39}\text{Ar}$ biotite ages should reflect cooling through $\sim 300^\circ\text{--}350^\circ\text{C}$ (Grove and Harrison 1996). The apatite and titanite fission-track and biotite $^{40}\text{Ar}/^{39}\text{Ar}$ ages for all intrusions agree within experimental error. Given the difference in closure temperatures, these results indicate that the intrusions cooled rapidly to near surface temperatures and were emplaced at high levels in the crust.

Apatites show a complex history of track retention as they cool from 120° to 60°C , a temperature range referred to as the partial annealing zone (PAZ). Variations in track lengths can be related to the cooling history of the apatite through the PAZ (Gleadow et al. 1983, 1986). Confined mean track lengths of $14\text{--}15\ \mu\text{m}$ indicate rapid cooling through the PAZ, whereas shorter mean track lengths of $12\text{--}13\ \mu\text{m}$ indicate slower cooling through the PAZ. Arne (1992) measured track lengths in apatite for three samples from the Magnet Cove complex and one sample from Granite Mountain. Mean track lengths for these samples varied from 14.69 ± 0.62 to $15.36 \pm 0.97\ \mu\text{m}$, indicating that these sam-

ples rapidly cooled through the PAZ. These relatively long mean track lengths support the inference that the intrusions were emplaced at high levels and rapidly cooled to near surface temperatures. Given the age concordance between the different dating methods and the previously determined radiometric ages (table 2) for the AAP, we conclude that the fission-track and $^{40}\text{Ar}/^{39}\text{Ar}$ ages reported here represent emplacement ages for the various intrusions.

Age Distribution. Best ages were determined for each of the intrusions using the $^{40}\text{Ar}/^{39}\text{Ar}$ and fission-track ages determined in this study, the $^{40}\text{Ar}/^{39}\text{Ar}$ ages of Baksi (1997), the K-Ar Prairie Creek lamproite age of Gogineni et al. (1978), and the Potash Sulfur Springs zircon U-Pb age of Zartman and Howard (1987). The distribution of these ages is shown in figure 3. There is a progression of decreasing age across the province, from lamproite in the west with an age of 106 Ma to syenites from Granite Mountain in the east with an 88-Ma age. Various authors (e.g., Duncan 1984; Baksi 1997) have suggested that the age distribution in the AAP represents a hotspot trace. The older ages for the lamproites at the western end of the province compared to the $\sim 16\text{-m.yr.}$ -younger age for the Granite Mountain syenite body at the eastern end of the

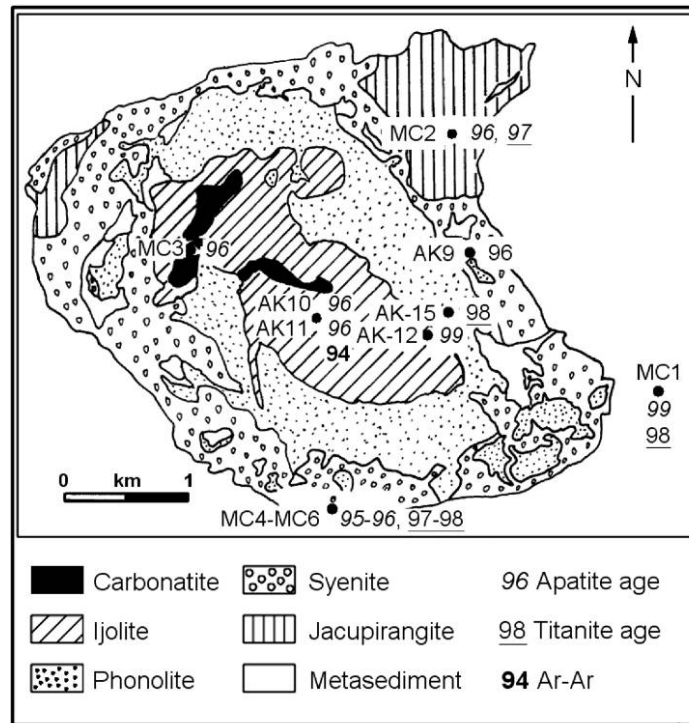


Figure 4. Geologic map of the Magnet Cove complex (after Erickson and Blade 1963) showing the location of the various samples and their fission-track and $^{40}\text{Ar}/^{39}\text{Ar}$ mica ages.

province does support the inference of a hotspot trace. However, the intervening intrusives range in age from 101 to 94 Ma and do not show a geographic trend (fig. 3). Note that the 100-Ma Benton dike swarm is in geographic close proximity to the 88-Ma Saline County nepheline syenite body, an observation contrary to the inference of a hotspot trace.

The ages vary with the petrology of the AAP intrusions. The oldest intrusions are lamproites (~106 Ma). The 101–94-Ma ages comprise the association carbonatites, lamprophyres, and a variety of silica-undersaturated rocks (jacupirangites, ijolites, nepheline syenites). The youngest intrusions (~88 Ma) are the large nepheline syenite bodies of Saline County and Granite Mountain. These nepheline syenites have geochemical characteristics distinctly different from the nepheline syenites found in the 101–94-Ma group (Eby 2000).

Isotopic Data. The existing isotopic data provide a useful insight into the petrogenetic history of the AAP. Re-Os and Sm-Nd isotopic data for the Prairie Creek lamproite (Lambert et al. 1995) yield non-radiogenic initial γ_{Os} (–3.2 to –3.6) and ϵ_{Nd} (–10) and depleted-mantle-model ages of 0.9–1.2 Ga, leading to the conclusion that the lamproite was

derived from a metasomatized Proterozoic subcontinental lithospheric mantle. Tilton et al. (1987) investigated the Sr, Nd, and Pb isotopic characteristics of carbonatites from Magnet Cove and Potash Sulfur Springs and syenites from Magnet Cove and Granite Mountain (and associated syenite bodies). For these intrusions, $\epsilon_{\text{Nd}} = +2.1$ to $+4.0$ and $\epsilon_{\text{Sr}} = -11.4$ to -14.6 (Magnet Cove only). The Pb isotopic values generally plot in the MORB-ocean island fields (although for some samples there was evidence of crustal contamination or mixing between different mantle domains). From these observations, Tilton et al. (1987) concluded that the magmas were derived from a large-ion-lithophile element-depleted mantle. Hence, the existing isotopic data suggest that the lamproites were extracted from a very different mantle than the rest of the magmas of the AAP. Recently obtained Sr, Nd, and Pb isotopic data (Duke et al. 2008) also support the contention that the lamproites were derived from subcontinental lithospheric mantle, while the other magmas were derived from asthenospheric mantle.

Petrogenetic Interpretation. Taking into account both the geochronological and isotopic data, the initial melts (the lamproites) were derived from the

Table 2. Other Radiometric Ages for the Arkansas Province

Locality	Technique used/ material dated/lithology	Age \pm 1 (Ma)	Source
Prairie Creek	K-Ar/phlogopite/lamproite	99 \pm 2, 108 \pm 3	Zartman 1977
Prairie Creek	K-Ar/phlogopite/lamproite	106 \pm 3	Gogineni et al. 1978
Magnet Cove	K-Ar/biotite/melteigite, ijolite	97 \pm 5, 100 \pm 5	Zartman et al. 1967
Magnet Cove	Rb-Sr/biotite/ijolite	102 \pm 8	Zartman et al. 1967
Magnet Cove	Fission track/apatite/unknown	97 \pm 7, 100 \pm 7, 104 \pm 4	Arne 1992
Magnet Cove	$^{40}\text{Ar}/^{39}\text{Ar}$ /biotite/ijolite, jacupirangite	94.4 \pm .2, 94.2 \pm .2	Baksi 1997
Magnet Cove	Fission track/apatite/carbonatite	90 \pm 9, 103 \pm 10	Scharon and Hsu 1969
Magnet Cove	Fission track/titanite/syenite	105 \pm 10	Scharon and Hsu 1969
Magnet Cove	K-Ar/whole rock/trachyte	102 \pm 4	Baldwin and Adams 1971
Potash Sulfur Springs	U-Pb/zircon/feldspathoidal syenite	100 \pm 2	Zartman and Howard 1987
Granite Mountain	K-Ar/biotite/nepheline syenite	89 \pm 4, 94 \pm 5	Zartman et al. 1967
Granite Mountain	Rb-Sr/biotite/nepheline syenite	89 \pm 3	Zartman et al. 1967
Granite Mountain	Fission track/apatite/syenite	88 \pm 6	Arne 1992
Granite Mountain	$^{40}\text{Ar}/^{39}\text{Ar}$ /biotite/syenite	89.6 \pm .5	Baksi 1997

Note. Where appropriate, the radiometric ages were recalculated using the decay constants recommended by Steiger and Jäger (1977).

subcontinental lithosphere. All the younger intrusions have an asthenospheric signature. Between 101 and 94 Ma, carbonatitic and various silica-undersaturated melts that originated in the mantle were emplaced at high levels in the crust followed by intrusion of the large nepheline syenite bodies (at ~88 Ma). Unlike the nepheline syenites associated with the older intrusions, the younger nepheline syenites have chemical characteristics (well-developed feldspar fractionation trends on Eu/Eu* vs. Sr and Ba diagrams, compositions that plot near the 1-bar eutectic in the Ne-Qtz-Ks system) that suggest extensive fractional crystallization at relatively low pressures from a mafic magma (Eby 2000). The size of the nepheline syenite bodies and the inferred extensive fractional crystallization requires greater melt volumes and presumably a more significant mantle input. Hence, the age progression in the AAP represents a change from a subcontinental lithospheric source to an asthenospheric source. Initial melts are derived from the subcontinental lithosphere followed by direct involvement of the asthenospheric mantle in melt generation. The inferred increase in melt volume with decreasing age suggests more extensive melting of the asthenospheric source with decreasing age.

Tectonic Setting—Hotspot versus Crustal Extension. Alkaline provinces are widely distributed in within-plate settings and occur throughout the last 2+ billion years of Earth's history (the current oldest known occurrence is the 2.68-Ga Sakharjok alkaline syenite complex, Kola Peninsula, Russia; Zozulya et al. 2005). The tectonic setting for these provinces is still a matter of debate. The two common, and competing, hypotheses are that alkaline

provinces are (1) the result of hotspot activity or (2) due to reactivation of earlier zones of crustal weakness caused by changes in the within-plate stress field. The reactivation of these zones of crustal weakness leads to decompression melting. As is the case for many geological debates, it is not unreasonable to suppose that both models may give rise to alkaline magmatism and the challenge is to determine which model applies to a particular case. The AAP is a typical example of the problem.

The generally accepted model for the formation of the APP is hotspot magmatism. Predicted Bermuda hotspot paths pass through or close to the AAP (Morgan 1983; Duncan 1984; Muller et al. 1993). The path predicted by Duncan (1984) passes directly through the AAP (fig. 3), while the other predicted paths are somewhat north (Morgan 1983) or south (Muller et al. 1993). The mid-Cretaceous volcanism that starts at ~115 Ma in eastern Kansas and ends at ~65 Ma in central Mississippi follows the projected Bermuda hotspot trace. The major geochronological controls are the 106–88-Ma ages for the AAP, the 81.9–65.5-Ma whole-rock $^{40}\text{Ar}/^{39}\text{Ar}$ ages for alkali basalt and phonolite from the Monroe uplift 200 km southeast of the AAP (Baksi 1997), and a whole-rock $^{40}\text{Ar}/^{39}\text{Ar}$ age of 64.0 \pm 1.5 Ma for phonolite (Baksi 1997) from the Jackson Dome, 350 km southeast of the AAP. This presumed path yields a plate motion of 20 mm yr⁻¹. Cox and Van Arsdale (1997, 2002), using multiple lines of reasoning, related the formation of the Mississippi embayment to the Bermuda hotspot. They argue for 1–3 km of mid-Cretaceous regional uplift and erosion that accompanies the passage of the hotspot. This is followed by subsidence that forms the Mississippi embayment. The latest version of

the geologic timescale (Gradstein et al. 2004) places the boundary between the Lower and Upper Cretaceous at 99.6 Ma, and thus emplacement of the various intrusive units in the AAP corresponds with this period of inferred uplift and erosion.

There are several arguments against the hotspot model. (1) The west–east distance from the 106-Ma lamproites to the 88-Ma Granite Mountain nepheline syenites is approximately 130 km. The plate motion estimated from this distance and age difference is $\sim 7 \text{ mm yr}^{-1}$, almost a factor of three less than the predicted rate. Additionally, the widespread occurrence of ages between 101 and 94 Ma without any apparent geographic trend does not support a hotspot trace. (2) In a carefully reasoned paper, Vogt and Jung (2007) conclude that the Bermuda rise was not the product of hotspot volcanism and that other conflicting time-space relationships for igneous activity throughout the southern United States negate the hotspot hypothesis.

The AAP lies along the extension of the Late Proterozoic–early Paleozoic Mississippi graben. The AAP also occurs in a pervasive zone of weak crust and is bounded by the extension of several transform faults (Thomas 2006). Mickus and Keller (1992), using seismic and gravity data, constructed a north-south lithospheric cross section that passes slightly to the west of the AAP. The deformed sedimentary rocks of the Ouachita orogeny (and Benton uplift) are found between Precambrian crust to the north (current depth to the Moho $\sim 40 \text{ km}$) and a microcontinental block to the south. Between these two continental blocks the Moho is found at a depth of $\sim 30 \text{ km}$. The boundary between low-density (3300 kg m^{-3}) mantle to the north and high-density mantle (3420 kg m^{-3}) to the south lies slightly south of the AAP. The inferred uplift (Cox and Van Arsdale 1997, 2002) of 1–3 km that occurred at the time of intrusion of the AAP is an important constraint on any model. If extension occurs in this region during the Cretaceous, we might expect crustal failure to occur in the area of the AAP, which could lead to the upwelling of asthenospheric mantle that provides both the heat and ultimately the material for AAP magmatism. Mantle upwelling in this region would also elevate the overlying crust that would then fracture along the zones of weakness providing conduits for the magmas. This localized extension would be unrelated to a long-duration hotspot. Some support for

this model is provided by the variation in time of the source of the melts, with the earlier melts derived from the subcontinental lithosphere and later melts from the asthenosphere indicating progression toward deeper melts with time.

Conclusions

Whole rock and mica $^{40}\text{Ar}/^{39}\text{Ar}$ and titanite and apatite fission-track ages indicate that the various intrusions of the AAP were emplaced between 106 and 88 Ma. The intrusion ages tend to decrease in a west to east direction, but similar ages are dispersed over a wide geographic area. The agreement between ages determined by the various methods, each of which has a different closing (or blocking) temperature indicates that the intrusions were emplaced at high levels and cooled quickly to ambient near-surface temperatures. A relationship between petrology and age exists in which the oldest intrusions are lamproites and are derived from a subcontinental lithospheric source while the younger intrusions are derived from asthenospheric mantle. Although one of the projected Bermuda hotspot traces passes through the AAP, the age progression within the AAP does not support a hotspot model. Additionally, recent studies have questioned the existence of the Bermuda hotspot (Vogt and Jung 2007). The AAP falls on the extension of the Mississippi graben and occurs between two continental blocks within a region of mid-Cretaceous uplift. It is proposed that the AAP formed in response to a regional extensional stress field that led to melting in the subcontinental lithospheric mantle and subsequent rise and melting of asthenospheric mantle.

ACKNOWLEDGMENTS

T. Armbrustmacher, E. M. Morris, and J. M. Howard assisted with the sample collection. Neutron irradiations were done at the University of Massachusetts Lowell Radiation Laboratory. Construction of the $^{40}\text{Ar}/^{39}\text{Ar}$ laboratory at the University of Queensland was partially funded by Australian Research Council Equipment Grant A39531815, and this project was funded by the University of Queensland Argon Geochronology in Earth Sciences laboratory (UQ-AGES). J. M. Howard and M. Roden-Tice are thanked for their careful and constructive reviews of the manuscript.

REFERENCES CITED

- Arbenz, J. K. 1989. The Ouachita system. *In* Bally, A. W., and Palmer, A. R., eds. *The geology of North America: an overview* (Vol. A). Boulder, CO, Geol. Soc. Am., p. 371–396.

- Arne, D. C. 1992. Evidence from apatite fission-track analysis for regional Cretaceous cooling in the Ouachita Mountain Fold Belt and Arkoma Basin of Arkansas. *Am. Assoc. Pet. Geol. Bull.* 76:392–402.
- Baksi, A. K. 1997. The timing of Late Cretaceous alkalic igneous activity in the northern Gulf of Mexico basin, southeastern USA. *J. Geol.* 105:629–643.
- Baldwin, O. D., and Adams, J. A. S. 1971. Potassium-40/argon-40 ages of the alkalic igneous rocks of the Balcones Fault trend of Tex. *Tex. J. Sci.* 22:223–231.
- Byerly, G. R. 1991. Igneous activity. *In* Salvador, A., ed. *The Gulf of Mexico Basin (Geology of North America, Vol. J)*. Boulder, CO, Geol. Soc. Am., p. 91–108.
- Cox, R. T.; and Van Arsdale, R. B. 1997. Hotspot origin of the Mississippi embayment and its possible impact on contemporary seismicity. *Eng. Geol.* 46:201–216.
- . 2002. The Mississippi Embayment, North America: a first-order continental structure generated by the Cretaceous superplume mantle event. *J. Geodyn.* 34:163–176.
- Duke, G. I.; Carlson, R. W.; and Eby, G. N. 2008. Two distinct sets of magma sources in Cretaceous rocks from Magnet Cove, Prairie Creek, and other igneous centers of the Arkansas alkaline province, USA. *EOS Trans. Am. Geophys. Union* 89(53), fall meeting 2008 supplement, abstract V31C-2169.
- Duncan, R. A. 1984. Age progressive volcanism in the New England seamounts and the opening of the central Atlantic Ocean. *J. Geophys. Res.* 89:9980–9990.
- Eby, G. N. 2000. Geochronology, geochemistry and petrogenesis of the Arkansas alkaline province. *Geol. Soc. Am. Abstr. Program* 32:A9.
- Erickson, R. L., and Blade, L. V. 1963. Geochemistry and petrology of the alkalic igneous complex at Magnet Cove, Arkansas. *U.S. Geol. Surv. Prof. Pap.* 425, 95 p.
- Fitzgerald, P. G., and Gleadow, A. J. 1988. Fission-track geochronology, tectonics and structure of the Transantarctic Mountains in northern Victoria Land, Antarctica. *Chem. Geol.* 73:1497–1502.
- Flohr, M. J. K., and Howard, M. 1994. Geochemical data of drill core samples of carbonatites and associated igneous rocks, Benton, Arkansas. *U.S. Geol. Surv. Open File Rep.* 94-450, 21 p.
- Gleadow, A. J. W.; Duddy, I. R.; Green, P. F.; and Lovering, J. F. 1986. Confined fission-track lengths in apatite: a diagnostic tool for thermal history. *Contrib. Mineral. Petrol.* 94:405–415.
- Gleadow, A. J. W.; Duddy, I. R.; and Lovering, J. F. 1983. Fission-track analysis: a new tool for the evaluation of thermal histories and hydrocarbon potential. *Aust. Petrol. Explor. Assoc. J.* 23:93–102.
- Gogineni, S. V.; Melton, C. E.; and Giardini, A. A. 1978. Some petrological aspects of the Prairie Creek diamond-bearing kimberlite diatreme, Arkansas. *Contrib. Mineral. Petrol.* 66:251–261.
- Gradstein, F. M.; Ogg, J. G.; Smith, A. G.; Bleeker, W.; and Lourens, L. J. 2004. A new geologic time scale with special reference to Precambrian and Neogene. *Episodes* 27:83–100.
- Grove, M., and Harrison, T. M. 1996. $^{40}\text{Ar}^*$ diffusion in Fe-rich biotite. *Am. Mineral.* 81:940–951.
- Hendricks, J. D. 1988. Bouguer gravity of Arkansas. *U.S. Geol. Surv. Prof. Pap.* 1474, 31 p.
- Hildenbrand, T. G. 1985. Rift structure of the northern Mississippi Embayment from the analysis of gravity and magnetic data. *J. Geophys. Res.* 90:12,607–12,622.
- Hurfurd, A. J. 1990. Standardization of fission track dating calibration: recommendation by the fission track working group of the I.U.G.S. Subcommittee on Geochronology. *Chem. Geol.* 80:171–178.
- Hurfurd, A. J., and Green, P. F. 1982. A user's guide to fission track dating calibration. *Earth Planet. Sci. Lett.* 59:343–354.
- . 1983. The zeta age calibration of fission-track dating. *Isot. Geosci.* 1:285–317.
- Kidwell, A. L. 1951. Mesozoic igneous activity in the northern Gulf Coastal Plain. *Trans. Gulf Coast Assoc. Geol. Soc.* 1:182–199.
- Lambert, D. D.; Shirey, S. B.; and Bergman, S. C. 1995. Proterozoic lithospheric mantle source for the Prairie Creek lamproites: Re-Os and Sm-Nd isotopic evidence. *Geology* 23:273–276.
- McCormick, G., and Heathcote, R. 1979. Mineralogy of the Morrilton alvikite dike, Conway County, Arkansas. *Geol. Soc. Am. Abstr. Program* 11:163.
- Mickus, K. L.; and Keller, G. R. 1992. Lithospheric structure of the south-central United States. *Geology* 20:335–338.
- Mitchell, R. H.; and Bergman, S. C. 1991. Petrology of lamproites. Dordrecht, Kluwer Academic, 440 p.
- Morgan, W. J. 1983. Hotspot tracks and the early rifting of the Atlantic. *Tectonophysics* 94:123–139.
- Morris, E. M. 1987. The Cretaceous Arkansas alkalic province: a summary of petrology and geochemistry. *In* Morris, E. M., and Pasteris, J. D., eds. *Mantle metasomatism and alkaline magmatism*. *Geol. Soc. Am. Spec. Pap.* 215:217–233.
- Muller, R. D.; Royer, J.-Y.; and Lawver, L. A. 1993. Revised plate motions relative to the hotspots from combined Atlantic and Indian ocean hotspot tracks. *Geology* 21:275–278.
- Naeser, C. W. 1981. The fading of fission-tracks in the geologic environment: data from deep drill holes. *Nucl. Tracks Radiat. Meas.* 5:248–250.
- Naeser, C. W., and Faul, H. 1969. Fission-track annealing in apatite and sphene. *J. Geophys. Res.* 74:705–710.
- Scharon, L., and Hsu, I. 1969. Paleomagnetic investigation of some Arkansas alkalic igneous rocks. *J. Geophys. Res.* 74:2774–2779.
- Steiger, R. H.; and Jäger, E. 1977. Subcommittee on geochronology: convention on the use of decay constants in geo- and cosmo-chronology. *Earth Planet. Sci. Lett.* 36:359–362.
- Thomas, W. A. 2006. Tectonic inheritance at a continental margin. *GSA Today* 16:4–11.
- Tilton, G. R.; Kwon, S. T.; and Frost, D. M. 1987. Isotopic relationships in Arkansas Cretaceous alkalic complexes. *In* Morris, E. M., and Pasteris, J. D., eds. *Mantle*

- metasomatism and alkaline magmatism. *Geol. Soc. Am. Spec. Pap.* 215:241–248.
- Vasconcelos, P. M.; Onoe, A. T.; Kawashita, K.; Soares, A. J.; and Teixeira, W. 2002. $^{40}\text{Ar}/^{39}\text{Ar}$ geochronology at the Instituto de Geociências, USP: instrumentation, analytical procedures, and calibration. *An. Acad. Bras. Cienc.* 74:297–342.
- Vogt, P. R., and Jung, W.-Y. 2007. Origin of the Bermuda volcanoes and Bermuda Rise: history, observations, models, and puzzles. *In* Foulger, G. R., and Jurdy, D. M., eds. *Plates, plumes and planetary processes*. *Geol. Soc. Am. Spec. Pap.* 430:553–591.
- Wagner, G. A. 1968. Fission-track dating of apatites. *Earth Planet. Sci. Lett.* 4:411–414.
- Zartman, R. E. 1977. Geochronology of some alkalic rock provinces in eastern and central United States. *Annu. Rev. Earth Sci.* 5:257–286.
- Zartman, R. E.; Brock, M. R.; Heyl, A. V.; and Thomas, H. H. 1967. K-Ar and Rb-Sr ages of some alkalic intrusive rocks from central and eastern United States. *Am. J. Sci.* 265:848–870.
- Zartman, R. E., and Howard, J. M. 1987. Uranium-lead age of large zircon crystals from the Potash Sulfur Springs igneous complex, Garland County, Arkansas. *In* Morris, E. M., and Pasteris, J. D., eds. *Mantle metasomatism and alkaline magmatism*. *Geol. Soc. Am. Spec. Pap.* 215:235–240.
- Zozulya, D. R.; Bayanova, T. B.; and Eby, G. N. 2005. Geology and age of the late Archean Keivy alkaline province, northeastern Baltic shield. *J. Geol.* 113:601–608.